JOURNAL OF CATALYSIS **140**, 395–405 (1993)

Electron Microscope Investigation of Mesopore Formation and Aluminum Migration in USY Catalysts

C. CHOI-FENG,[1] J. B. HALL, B. J. HUGGINS, AND R. A. BEYERLEIN

Amoco Research Center, P.O. Box 3011, Naperville, Illinois 60566

Received June 30, 1992; revised September 17, 1992

Combined high resolution electron microscope (HREM) and analytical electron microscope (AEM) investigations have been used to study the formation and evolution of mesopores in hydrothermally dealuminated ultrastable Y (USY) materials. The HREM results give clear evidence for an inhomogeneous formation and distribution of the 5- to 50- nm defect regions attributed to mesopores. Such features are characteristic of extended hydrothermal treatment. In regions with high defect concentration, mesopores coalesce to form channels and cracks, which ultimately define the boundaries of fractured crystallite fragments. At these boundaries, a dark band is often observed which is highly enriched in aluminum, while within the mesopore itself, aluminum appears to be deficient. These dark bands are observed both in a neat USY material subjected to several cycles of steam/acid treatment and in a high-temperature steam-deactivated USY fluid catalytic cracking (FCC) catalyst. Individual grains of both the neat USY and the dealuminated USY catalyst exhibit extreme fracturing into small crystallites of dimensions 20 to 50 nm. The fracturing is attributed to the nonequilibrium nature of the high-temperature steam treatments which characterizes accelerated deactivation procedures in the laboratory. © 1993 Academic Press, Inc.

INTRODUCTION

The catalytic properties of ultrastable Y (USY) zeolite are directly influenced by the zeolite destruction which occurs during formation of USY and during subsequent hydrothermal treatment. For example, it has been suggested that the internal channels associated with mesopore formation provide greater accessibility to the micropore system defined by the crystalline zeolite. Yet, little information is available regarding mechanisms of mesopore formation and evolution. The nature and role of nonframework Al that is associated with mesopore formation are also poorly understood.

Previous transmission electron microscope (TEM) studies of hydrothermal aging of neat USY materials (*1–5*) and also of USY cracking catalysts (*6–9*) have shown 5–50 nm defect domains, which were attributed to mesopores. Such features, which become more pronounced in the presence of vanadium (*6, 7*), are characteristic of extended hydrothermal treatment. Scherzer (*10, 11*) and Maugé *et al.* (*5*) have suggested that these regions of zeolite destruction comprise the silica source for "healing" the tetrahedral site vacancies left by hydrothermal dealumination (*12, 13*). Sorption studies (*14, 15*) are consistent with the picture of entire sodalite units being destroyed concomitant with the rebuilding or healing of the USY framework. Typical porosity analyses of mildly steamed USY materials show a distribution of mesopore dimensions in the range 5–50 nm, that is, skewed toward the smaller sizes (*2, 4*), further supporting the association of the light "amorphous" zones observed by TEM with the secondary pore system characteristic of USY materials.

Previous studies of USY materials subjected to extended hydrothermal treatment have suggested a homogeneous (*2*) or near homogeneous (*3, 4*) distribution of mesopores. In contrast, recent investigations on a hydrothermally aged La–Y cracking cata-

---

[1] To whom correspondence should be addressed.

0021-9517/93 $5.00

lyst (*8*) demonstrate significant inhomogeneity both in the extent of dealumination and in defect formation.

In the present study, both high resolution electron microscopy (HREM) and analytical electron microscopy (AEM) are utilized to track the formation and evolution of mesopores, and the ultimate fate of the associated extralattice Al in hydrothermally treated USY materials. Results for a laboratory steamed neat USY material and for a high-temperature steam deactivated USY fluid catalytic cracking (FCC) catalyst are compared with each other, and with results from a previous study on age-separated equilibrium USY cracking catalyst from the fluid cracking unit (FCU) (*9*).

EXPERIMENTAL

A highly dealuminated zeolite Y material was prepared by subjecting a sample of commercial high silica Y, LZ-Y82 from Union Carbide, to three cycles of steam/acid treatment in which each aqueous treatment was followed by rinsing and drying steps. The first cycle consisted of 600°C steam for 2 h, ammonium exchange using 1.8 *M* NH_4Cl, 65°C, 1.5 h, and then a mild acid treatment using 100 volumes of 0.033 *N* HCL, for 4 h at room temperature. The product material was given a second steam treatment at 650°C for 3 h, followed by two successive acid treatments using 50 volumes of 0.1 *N* HCl. A third steam treatment was carried out at 650°C for 4 h, followed by an acid treatment with 0.1 *N* HCl, and finally calcining at 538°C for 3 h. All steam treatments were carried out using 100% steam. A second highly dealuminated ultrastable Y material was prepared by steam treatment of a commercial fluid catalytic cracking catalyst, KOB-619-1A, obtained from Akzo (Ketjen Catalysts), at 816°C for 24 h using 100% steam in a fluidized bed. Properties of these two dealuminated USY materials after steam treatments are given in Table 1.

The as-prepared samples were ground to a fine powder, embedded in LR-White acrylic resin, and then cut with a diamond knife on a Reichert–Jung Ulracut E ultramicrotome to obtain thin sections approximately 60–80 nm thick. The sections were supported on Cu grids and coated lightly with C to gain conductivity. High-resolution electron microscopy (HREM) and analytical electron microscopy (AEM) were used to characterize the prepared

TABLE 1

Properties of Dealuminated USY Materials

	Steam/acid treated neat USY material[a]	Steam-treated USY cracking catalyst[b]
Surface area (m^2/g)		
Total	529	169
Pores < 2 nm diam.	436	117
Micropore vol. (cm^3/g)	0.21	0.057
% Cryst., relative to fresh	75	61[c]
Unit cell size (nm)	2.426	2.424
Framework Al/unit cell[d]	4.3 ± 1.1	2.0 ± 1.1

[a] The fresh USY parent material (LZ-Y82) showed a micropore volume of 0.26 cm^3/g and a unit cell size of 2.456 nm.

[b] The fresh parent USY FCC cracking catalyst (Ketjen KOB-619-1A) showed a micropore volume of 0.091 cm^3/g and a unit cell size of 2.440 nm.

[c] The crystallinity of the parent (fresh) catalyst relative to LZ-Y82, determined by X-ray diffraction, was 35%.

[d] Calculated from unit cell size correlation given by Kerr, G. T., *Zeolites* **9**, 350 (1989).

samples. For HREM, two microscopes, a JEOL JEM 2000EX and a JEOL JEM 2010, were used. The AEM work was done using a Noran TN5500 energy dispersive X-ray spectrometry (EDXS) attached to the Philips 420T scanning transmission electron microscope (STEM).

RESULTS

Steam/Acid Treated Neat USY Material

A TEM micrograph of a few steam/acid treated USY grains is shown in Fig. 1a. The mesopores appear as light pseudospherical domains, approximately 15 to 50 nm in dimension, corresponding to lower density. Although these domains have lost much of their crystallinity, the connecting regions remain crystalline (Fig. 1b). These light, low-crystallinity domains have been observed previously by many researchers and are referred to as the secondary pore system or mesopores (*1–5*). The mesopores, evident in most of the USY grains, are inhomogeneously distributed. Some grains appear to contain more mesopores than others; within individual grains, mesopores are often highly concentrated in localized regions. In regions of high concentration, mesopores appear to coalesce to form channels as seen in Fig. 1a. Such channels can apparently evolve into cracks, leading to the fracturing of the USY grains into several smaller fragments, as shown in Fig. 2. In extreme cases, the original large crystals have broken into crystallites as small as 20 nm. These small crystallites, each with a different crystallographic orientation, are shown in Fig. 3.

A STEM image of several USY grains, along with EDXS spectra of the entire imaged area (overall) and of two USY grains (PF1 and PF2), are shown in Fig. 4. Numerous mesopores are readily seen in grain 1 (PF1) while grain 2 (PF2) is largely free of mesopores. The average Si/Al ratio of the overall imaged area is lower than that of PF1, but higher than that of PF2. These results indicate that the formation of mesopores in the USY zeolite occurs concomitantly with its dealumination.

HREM investigation of the extensively dealuminated USY material shows characteristic "dark bands" within the channels or cracks that evolve from coalesced mesopores (Fig. 2). A STEM image of several similar USY grains along with three EDXS spectra are shown in Fig. 5. One spectrum was collected while scanning the partial field, PF1, a second with a stationary electron probe on a dark band (S-1), and a third with a stationary electron probe within a mesopore (S-2). From the spectra, it is evident that the dark band (S-1) is highly enriched in Al, while the mesopore itself shows a slight Al deficiency, with a slightly higher Si/Al than that for PF1. These narrow regions of enriched Al are resistant to mild acid treatment. They appear to represent an ultimate fate of the high-temperature steam-induced migration of nonframework Al, following its ejection from the crystalline lattice. An EDXS spectrum from an arbitrary location within an individual USY grain, S-3 (not shown), shows a Si/Al equivalent to that of PF1.

Steamed USY Catalyst

The USY grains are well mixed with the matrix in the steamed USY cracking catalyst. A transmission electron microscope (TEM) image of the overall structure of this sample is shown in Fig. 6. The amorphous matrix is evidenced as large lighter regions, while the crystalline (USY) grains are more dense. As in all low-magnification TEM images, cracks induced by the ultramicrotoming are readily seen as fracture lines approximately parallel to each other. Mesopores are revealed as lighter domains, typically concentrated in the interior of the grains. Some grains appear to have fewer mesopores than others. In comparison with the steam/acid treated net USY material, the USY cracking catalyst sample shows a greater departure from homogeneity with fewer mesopores overall. It is surprising that, within the USY catalyst sample, some

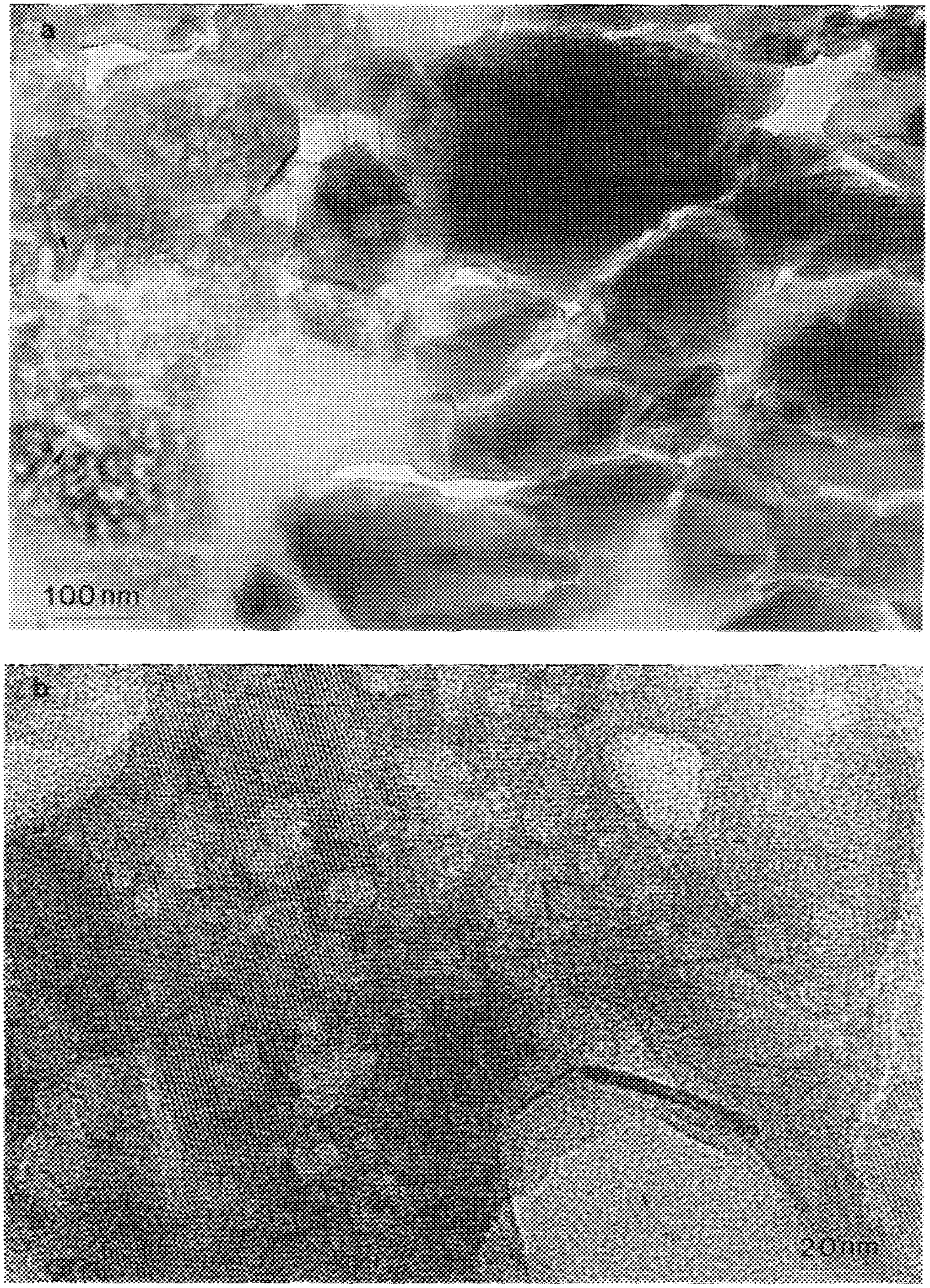

FIG. 1. (a) TEM image of a few steam/acid treated USY grains. An inhomogeneous distribution of mesopores is seen within individual grains; some grains contain more mesopores than others. In regions with high mesopore concentration, the pores coalesce to form channels (as indicated by arrows). (b) HREM image of steam/acid treated USY grains. Many mesopores are formed. Although localized disorder is observed within the pores, the connecting regions remain crystalline.

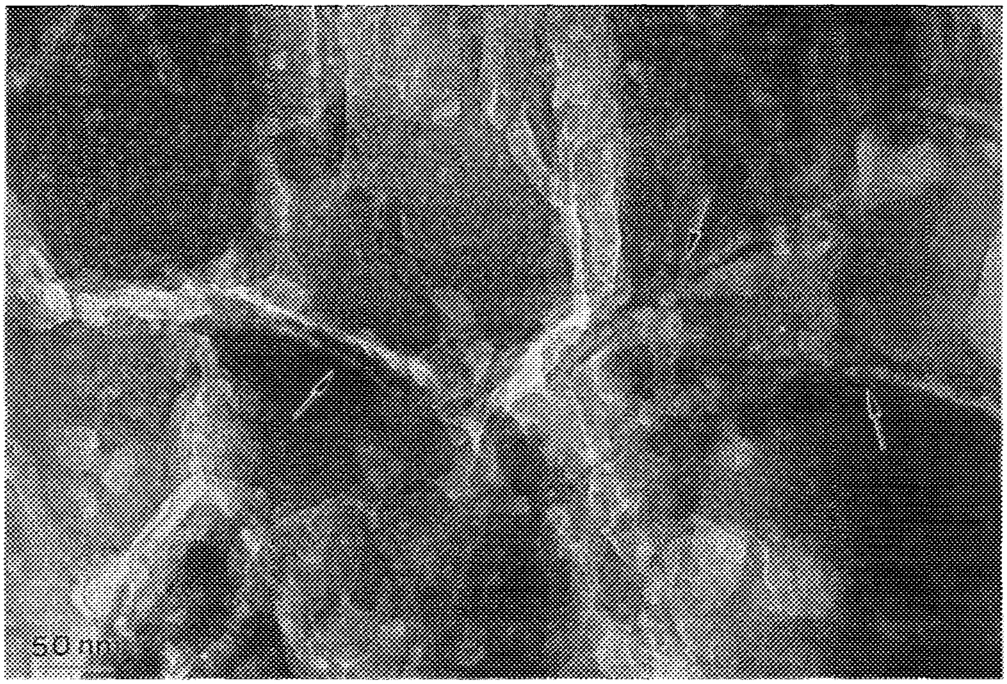

FIG. 2. HREM image of a steam/acid treated USY grain. Cracks (as indicated by arrows) are formed from the evolution of the coalesced mesopores. Dark bands are seen along these cracks.

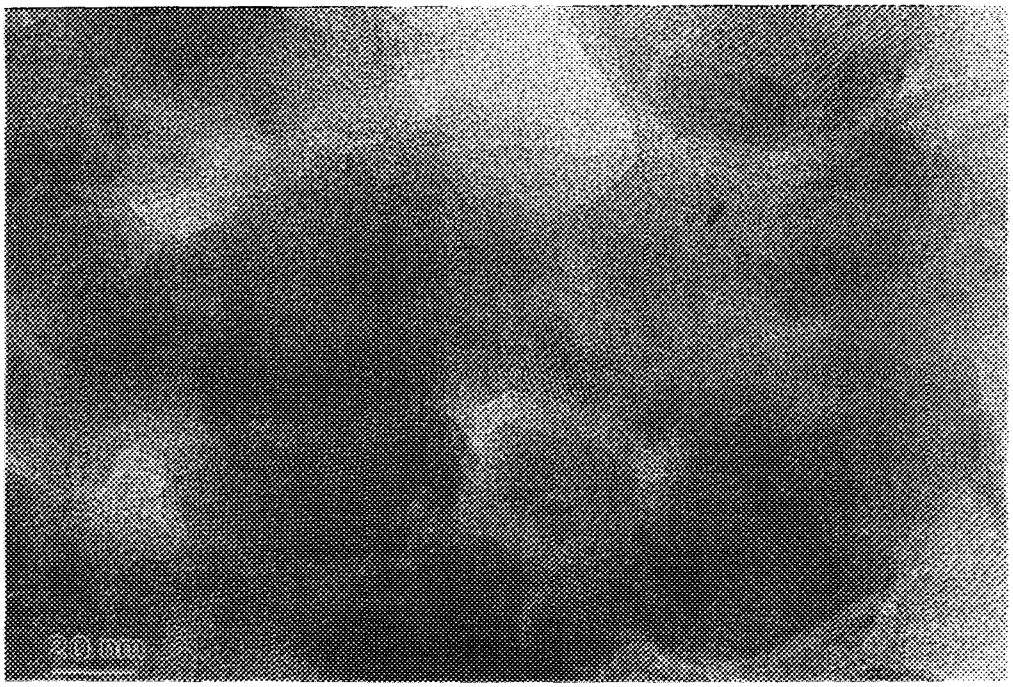

FIG. 3. HREM image showing a region where a steam/acid treated USY grain has broken into many small crystallites. Each crystallite has a different crystallographic orientation.

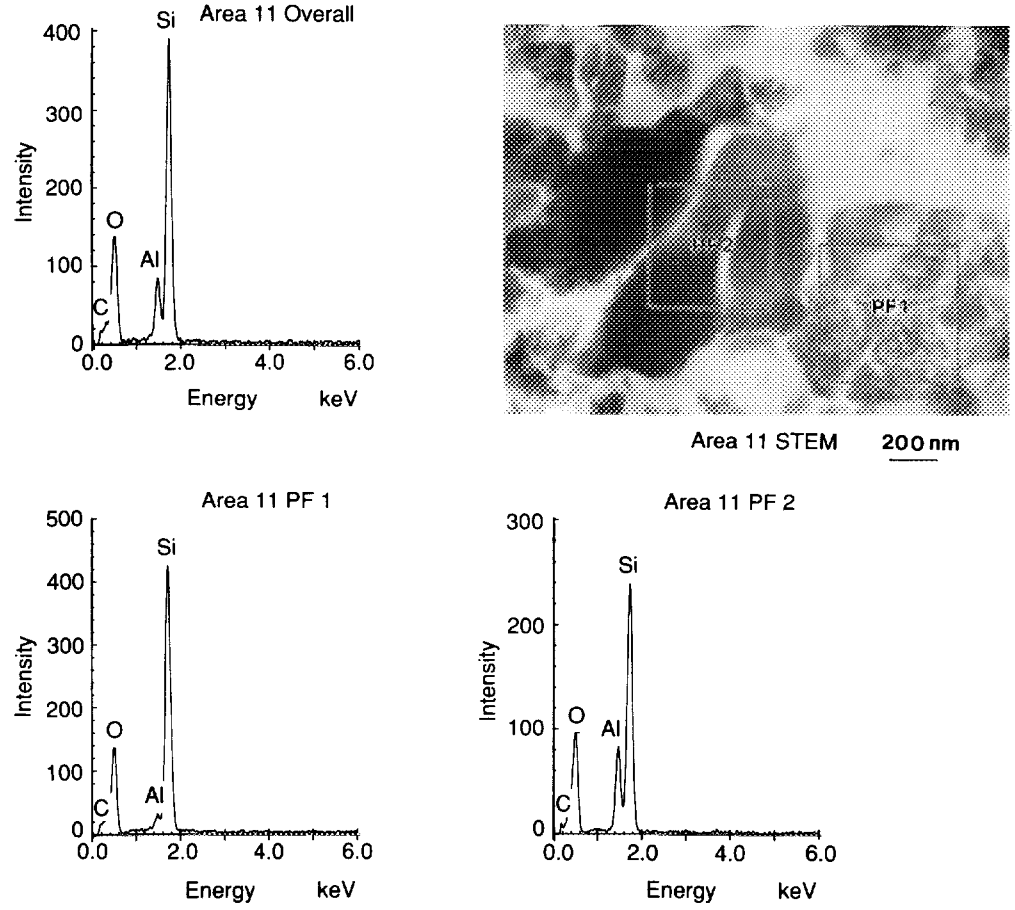

FIG. 4. STEM image of a few steam/acid treated USY grains along with EDXS spectra of the entire imaged area (overall) and two individual grains (PF1 and PF2). The grain shown in PF1 contains a high density of mesopores and has a higher Si/Al ratio than the average value (overall). The grain shown in PF2 is largely free of mesopores and has a lower Si/Al ratio than the average value.

grains exhibit a significantly lower incidence of defects than others (Fig. 6), since all microspheroidal catalyst particles are subjected to very similar conditions during the fluidizing steam treatment.

Detailed analyses of HREM images of the USY catalyst sample showed features similar to those seen in the steam/acid treated neat USY material. Low-density mesopores, 15 to 50 nm in dimension, are clearly seen in the USY grains in Fig. 6. In regions with high mesopore concentration, cracks have evolved from the coalesced mesopores, as seen in Fig. 7.

In contrast to the large cracks produced by ultramicrotoming (Fig. 6), the cracks which evolve from coalescence of mesopores (Fig. 7) show no preferred orientation. In addition there is a dark band associated with each mesopore-induced crack. These dark bands are Al enriched, similar to those observed in the steam/acid treated neat USY sample. The several small crystals seen in Fig. 7 have broken from a single original USY grain. From inspection of the lattice patterns, it is apparent that some crystal fragments remain in the same orientation while others have rotated slightly

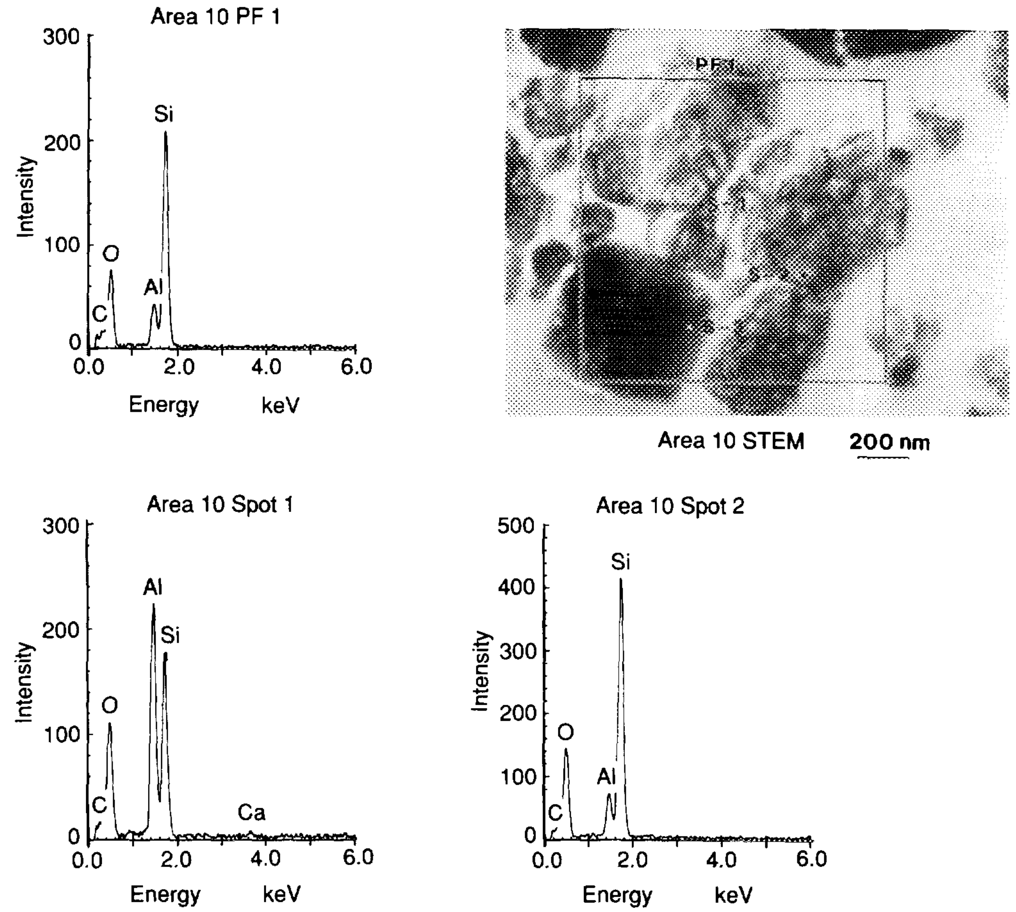

FIG. 5. STEM image of a few steam/acid treated USY grains along with EDXS spectra from three USY grains (PF1) and from a point on a dark band (S-1) and a point within a mesopore (S-2). The dark bands are found to be highly enriched in Al; within mesopores, Al is slightly deficient.

from their original orientation, probably due to relaxation of strain created by the extraction of framework Al. In some regions, evidence of extreme fracturing is observed, resulting in crystallites of only 20 to 50 nm in size, as shown in Fig. 8.

DISCUSSION

Consistent with previous TEM studies, the present work demonstrates that hydrothermal dealumination of zeolite Y, with or without subsequent acid treatment, leads to the formation of mesopores (*1–9*). Contrary to the reports by Patzelová and Jaeger (*2*), and by Lynch *et al.* (*3*, *4*), the present investigations of hydrothermally aged USY materials give clear evidence for an inhomogeneous distribution of mesopores. For neat USY materials, a marked inhomogeneity in the extent of dealumination and concomitant zeolite destruction was observed among different USY grains. Individual grains showed a markedly inhomogeneous distribution of mesopores or defects. Such inhomogeneities were even more pronounced for a higher temperature steam-deactivated commercial USY cracking catalyst.

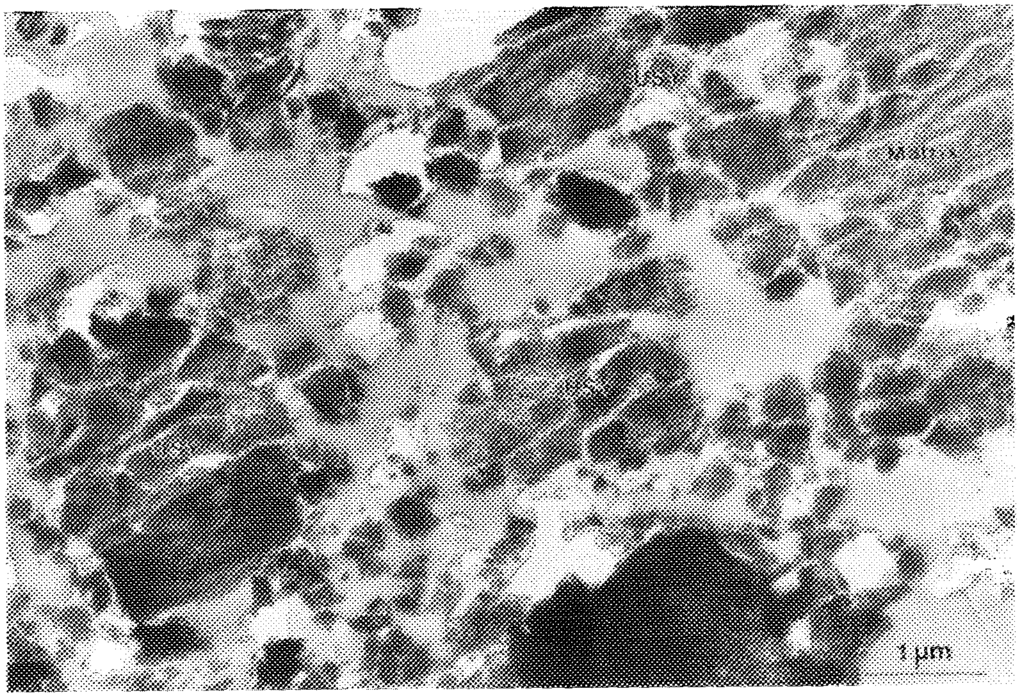

FIG. 6. TEM image showing the overall structure of the steamed USY catalyst. The matrix appears as regions of amorphous material, the USY zeolite as denser crystalline particles (as indicated). Mesopores are seen as lighter domains inside the USY grains. Large cracks due to ultramicrotoming are seen as fracture lines that are approximately parallel to each other.

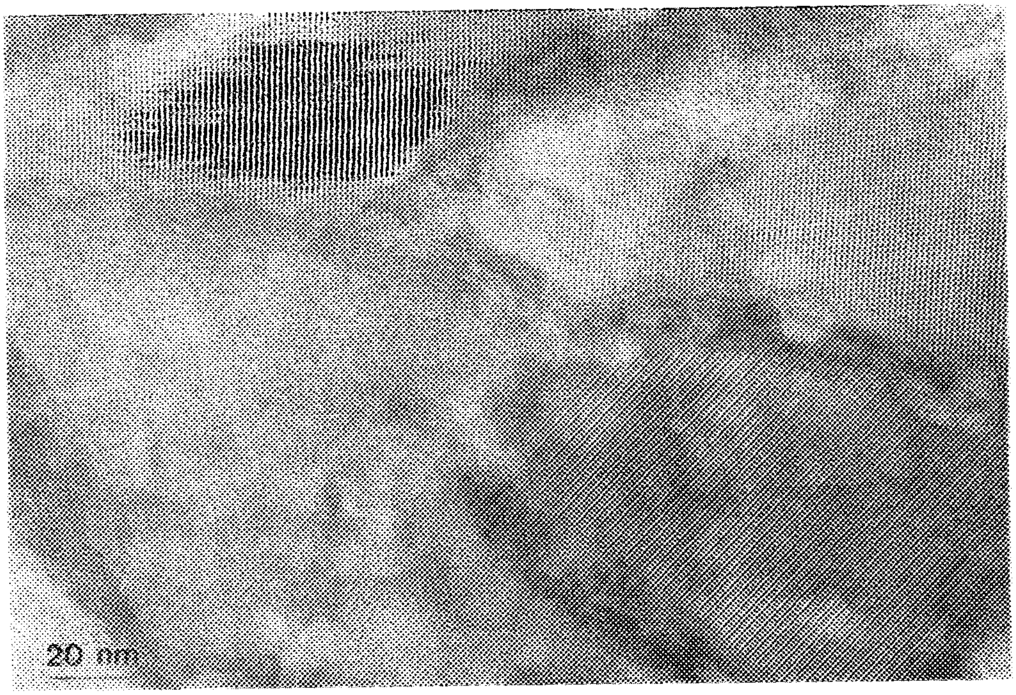

FIG. 7. HREM image showing the fracturing of a USY grain in the steamed USY catalyst. Each fractured crystallite is bounded by cracks evolved from coalescence of mesopores. The dark band seen along each crack is Al enriched, similar to those observed in the steam/acid treated neat USY material.

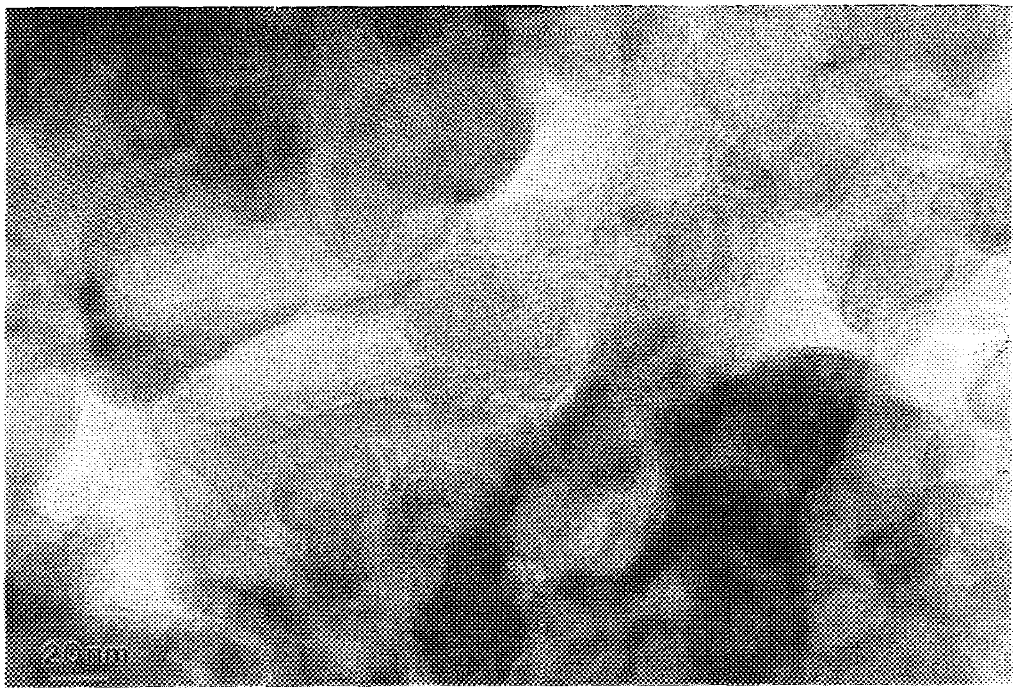

FIG. 8. HREM image showing the extreme case of zeolite fracturing caused by high-temperature steam treatment of the USY catalyst. Numerous small crystallites, as small as 20 nm in dimension, have broken away from an originally large single crystal.

The pronounced inhomogeneity in the character of defect formation may be a direct result of the accelerated, laboratory aging procedures. Such inhomogeneity might be expected since the dealumination by high-temperature steam treatment is an accelerated, nonequilibrium process. Ejection of framework Al and subsequent zeolite stabilization require significant migration of Al and Si, each of which is a rate-controlled process. Increased severity of hydrothermal treatment leads to a more rapid dealumination/fracturing, a further departure from equilibrium, and an even more inhomogeneous distribution of defects. This accounts for the more pronounced inhomogeneities in patterns of defect distribution in the steam-treated USY cracking catalyst. The extent to which the supporting matrix (for the USY catalyst) or the acid treatment following steaming (for the neat USY material) are important factors is beyond the scope of this study.

The present HREM observations provide new insights into the formation and evolution of mesopores which lead to extensive crystallite fracturing. In regions with high defect concentration, mesopores coalesce to form channels and cracks, which ultimately lead to crystallite fracture. For the laboratory steam treatments employed in these studies, this defect-induced fracture mechanism appears to comprise the primary route to crystallite size reduction, which for extended steam treatment, can lead to crystallite fragments as small as 20 nm. Similarly small crystallite fragments were reported in a recent study of age separated "equilibrium" catalyst from a commercial FCU (*9*). In this case, the small crystallites found within an "old" fraction were not demarcated by fracture boundaries (*9*), raising the possibility that, for the slower catalyst deactivation in the FCU, mechanisms other than defect-induced fracture are important in crystallite size reduction.

The fate of the ejected framework Al has been investigated previously by Ward and Lunsford (*16*) and also by Gross *et al.* (*17*). Under influence of high-temperature steam treatment, a significant surface enrichment of Al was observed, which was presumed to be associated with the migration of nonframework Al toward the crystallite surface. Ward and Lunsford found that this surface enrichment persisted following removal of up to half of the surface aluminum by NaOH (*16*). Gross *et al.* concluded that this surface enrichment was comprised of neutral species (*17*). Neither study was able to demonstrate whether this surface enrichment encompassed a concentration profile within a crystal grain or was solely comprised by a separate, presumably amorphous phase decorating the surface of the grain. More recently, Gélin and Courières (*8*) reported that, based on STEM analysis of a steamed La–Y catalyst, no significant aluminum concentration profile was observed within an individual grain. Instead, a pronounced increase in aluminum concentration was observed at defects, described as "dark lines," within the zerolite crystals.

In the present study, regions with high mesopore concentration are found to be aluminum deficient, indicating that framework dealumination and subsequent Al migration occurs concomitantly with mesopore formation. For extended hydrothermal treatment, the predominant fate of aluminum ejected from lattice sites appears to be closely associated with the dark bands, where Al is found to be highly enriched. In contrast to the observation by Gélin and Courières (*8*), our studies show that these noncrystalline aluminum-enriched regions are located not at the internal defects, but at or near newly formed fracture boundaries. These features are observed both for the steamed USY cracking catalyst and for the steam/acid treated neat USY zeolite, consistent with previous studies that found the surface enrichment of Al to persist through aqueous treatments which removed substantial amounts of aluminum (*16*).

CONCLUSIONS

The present HREM and AEM study of a steam/acid treated neat USY material and of a high-temperature steam treated USY cracking catalyst gives clear evidence for an inhomogeneous formation of mesopores which occurs concomitantly with a further zeolite dealumination. Such inhomogeneities are more pronounced for materials that are steam treated at a higher temperature and they are observed among different USY grains as well as within single grains. In regions with high defect concentration, mesopores coalesce to form channels and cracks, which ultimately define the boundaries of fractured crystallite fragments. At these boundaries, a dark band is often observed which is highly enriched in aluminum, while within the mesopore itself Al appears to be deficient. Some grains exhibit extreme fracturing into small crystallites of dimensions of 20 to 50 nm. These observations have, for the first time, provided insights into how the formation and evolution of mesopores lead to significant zeolite crystallite fracturing and concomitant Al migration in USY materials subjected to severe hydrothermal treatments.

The characteristics observed in the present study are clearly different than those observed by TEM in a previous study of age-separated equilibrium catalyst from a commercial FCU. For an "old" fraction of age-separated equilibrium catalyst, defects are less inhomogeneously distributed than for the lab-steamed USY catalyst, and the small crystallites remaining are not demarcated by fracture boundaries, suggesting that the mechanisms of deactivation are different for the slower catalyst deactivation in the FCU.

ACKNOWLEDGMENTS

The authors gratefully acknowledge Mr. John Newbury for performing the steam/acid treatments on the neat USY material and the high-temperature steam deactivation of the commercial USY cracking catalyst.

The authors express their gratitude to Professor N. Otsuka at Purdue University, W. Lafayette, IN, and to the staff at JEOL USA Application Laboratory, Peabody, MA, for the opportunity to use their high-resolution electron microscopes.

REFERENCES

1. Maugé, F., Auroux, A., Courcelle, J. C., Engelhard, Ph., Gallezot, P., and Grosmangin, J., *in* "Catalysis by Acids and Bases" (B. Imelik *et al.*, Eds.), p. 91. Elsevier, Amsterdam, 1985.
2. Patzelová, V., and Jaeger, N. I., *Zeolites* **7,** 240 (1987).
3. Lynch, J., Raatz, F., and Dufresne, P., *Zeolites* **7,** 333 (1987).
4. Lynch, J., Raatz, F., and Delalande, Ch., *in* "Characterization of Porous Solids" (K. K. Unger *et al.*, Eds.), p. 547. Elsevier, Amsterdam, 1988.
5. Maugé, F., Courcelle, J. C., Engelhard, Ph., Gallezot, P., Grosmangin, J., Primet, M., and Trasson, B., *in* "Zeolites, Synthesis, Structure, Technology, and Application" (B. Držaj *et al.*, Eds.), p. 401. Elsevier, Amsterdam, 1985.
6. Maugé, F., Courcelle, J. C., Engelhard, Ph., Gallezot, P., and Grosmangin, J., *in* "New Developments in Zeolite Science and Technology" (Y. Murikami *et al.*, Eds.), p. 803. Elsevier, Amsterdam, 1986.
7. Gallezot, P., Feron, B., Bourgogne, M., and Engelhard, Ph., *in* "Zeolites: Facts, Figures, Future" (P. A. Jacobs *et al.*, Eds.), p. 1281. Elsevier, Amsterdam, 1989.
8. Gélin, P., and Courières, T. Des, *Appl. Catal.* **72,** 179 (1991).
9. Beyerlein, R. A., Tamborski, G. A., Marshall, C. L., Meyers, B. L., Hall, J. B., and Huggins, B. J., *in* "Fluid Catalytic Cracking II" (M. L. Occelli, Ed.), ACS Symposium Series, Vol. 452, p. 109. American Chemical Society, Washington, DC, 1991.
10. Scherzer, J., *in* "Catalytic Materials—Relationship Between Structure and Reactivity" (T. E. Whyte *et al.*, Eds.), p. 157. American Chemical Society, Washington DC, 1984.
11. Scherzer, J., "Octane-Enhancing Zeolite FCC Catalysts: Scientific and Technical Aspects." Marcel Dekker, New York, 1990. See also Scherzer, J., *Catal. Rev.-Sci. Eng.* **31,** 254 (1989).
12. Maher, P. K., Hunter, F. D., and Scherzer, J., *Adv. Chem. Ser.* **101,** 266 (1971).
13. McDaniel, C. V., and Maher, P. K., *in* "Zeolite Chemistry and Catalysis; ACS Monograph 171" (J. A. Rabo, Ed.), p. 285. American Chemical Society, Washington, DC 1976.
14. Lohse, U., Stach, H., Thamm, H., Schirmer, W., Isirikjan, A. A., Regent, N. I., and Dubinin, M. M., *Z. Anorg. Chem.* **460,** 179 (1980).
15. Stach, H., Lohse, U., Thamm, H., and Schirmer, W., *Zeolites* **6,** 74 (1986).
16. Ward, M. B., and Lunsford, J. H., *J. Catal.* **87,** 524 (1984).
17. Gross, Th., Lohse, U., Engelhardt, G., Richter, K. H., and Patzelová, V., *Zeolites* **4,** 25 (1984).